Critical phenomena at a first-order phase transition in a lattice of glow lamps: Experimental findings and analogy to neural activity

Ludovico Minati, Antonio de Candia, and Silvia Scarpetta

Citation: Chaos **26**, 073103 (2016); doi: 10.1063/1.4954879
View online: http://dx.doi.org/10.1063/1.4954879
View Table of Contents: http://scitation.aip.org/content/aip/journal/chaos/26/7?ver=pdfcov
Published by the AIP Publishing

Critical phenomena at a first-order phase transition in a lattice of glow lamps: Experimental findings and analogy to neural activity

Ludovico Minati,[1,2,a)] Antonio de Candia,[3,4] and Silvia Scarpetta[4,5]
[1]*Center for Mind/Brain Sciences, University of Trento, 38123 Mattarello, Italy*
[2]*Complex Systems Theory Department, Institute of Nuclear Physics, Polish Academy of Sciences, Kraków, Poland*
[3]*Department of Physics "E. Pancini," University of Naples "Federico II," Napoli, Italy*
[4]*INFN Gr. Coll. Salerno, Unità di Napoli, Napoli, Italy*
[5]*Department of Physics "E.R.Caianiello," University of Salerno, Napoli, Italy*

(Received 28 March 2016; accepted 10 June 2016; published online 1 July 2016)

Networks of non-linear electronic oscillators have shown potential as physical models of neural dynamics. However, two properties of brain activity, namely, criticality and metastability, remain under-investigated with this approach. Here, we present a simple circuit that exhibits both phenomena. The apparatus consists of a two-dimensional square lattice of capacitively coupled glow (neon) lamps. The dynamics of lamp breakdown (flash) events are controlled by a DC voltage globally connected to all nodes via fixed resistors. Depending on this parameter, two phases having distinct event rate and degree of spatiotemporal order are observed. The transition between them is hysteretic, thus a first-order one, and it is possible to enter a metastability region, wherein, approaching a spinodal point, critical phenomena emerge. Avalanches of events occur according to power-law distributions having exponents ≈3/2 for size and ≈2 for duration, and fractal structure is evident as power-law scaling of the Fano factor. These critical exponents overlap observations in biological neural networks; hence, this circuit may have value as building block to realize corresponding physical models. *Published by AIP Publishing.*
[http://dx.doi.org/10.1063/1.4954879]

Recent work has shown that networks of non-linear electronic oscillators can recapitulate diverse aspects of neural dynamics, such as formation of complex synchronization patterns, offering opportunities to draw parallels between emergence in biological and engineered systems. However, two pervasive properties found across brains and *in-vitro* neuronal cultures have not been extensively addressed in circuit models: criticality, intended as operation at the boundary between ordered and disordered dynamical phases, and metastability, that is, the ability to maintain and switch between states having finite lifetime. Here, we investigated a network of glow lamps, a common type of neon-argon discharge tube, coupled in a two-dimensional square lattice by capacitors. We find that the system can be metastable with respect to the transition between two dynamical phases having different degrees of spatiotemporal order. Close to the spinodal points, which denote the limits of existence of the metastable states, fractal temporal structure emerges and activity avalanches are generated, whose size and duration follow power-law distributions having exponents ≈3/2 and ≈2. Despite differences in system scale, topology, and nature, these critical exponents overlap neural recordings; hence, this setup deserves consideration as building block to realize corresponding physical electronic models. The circuit is also of interest as a physical system wherein critical phenomena are observed close to the spinodal in a first-order phase transition.

I. INTRODUCTION

The dynamics of neural systems are pervaded by non-linear processes, apparent across micro-, meso-, and macroscopic scales ranging from single neurons to entire brains, which represent an essential substrate for homeostasis and behaviour. Critical phenomena and metastability, in particular, are deemed central to the emergence of cognitive processes.[1,2]

Experimental data and simulations indicate that biological neural networks preferentially operate in a regime characterized by the absence of characteristic time or length scale, as found at the critical point in thermodynamical systems.[3] Neural activity, whether recorded from cultured dissociated neurons, isolated slices, or intact brains, often features avalanches of events (spikes) whose size and duration distributions follow power laws with universal exponents, and long-range temporal correlations.[2,4–9] Near-critical dynamics are hypothesized to confer functional advantages such as maximizing dynamic range in response to external stimuli (e.g., in the ear), and enhancing information capacity by enlarging the repertoire of available activity patterns.[10–14] By positing an emergent internal mechanism driving the control parameter to the critical point, the paradigm of self-organized criticality offers a mechanistic explanation of how

[a)]Author to whom correspondence should be addressed. Electronic addresses: lminati@ieee.org, ludovico.minati@unitn.it, and ludovico.minati@ifj.edu.pl. Tel.: +39 335 486 670. URL: http://www.lminati.it

neural systems could maintain operation close to it in spite of countless perturbations.[15–17]

On the other hand, metastability is evident in the brain's innate ability to maintain persistent activity and switch between states having long but finite lifetime, which is necessary for functional integration and working memory.[1,18,19] Metastable states are again detectable in experimental data across different scales, particularly in electroencephalographic data, and appear in a multitude of neural models possessing a landscape of multiple attractors, some of which can also show critical phenomena.[18–21]

The precise relationship between these two aspects of neural dynamics remains elusive, but it has been postulated that criticality could maximize the number of available metastable states.[22–24]

Recently, renewed interest in neuromorphic electronic circuits has led to attempts to recapitulate select features of neural dynamics in experimental networks of physical oscillators, with the aim of drawing comparisons between the brain and other systems, and of complementing computational work with experimental data acquired in settings allowing more extensive manipulation compared to biological preparations. Promising results have been obtained with coupled chaotic oscillators; however, to the authors' knowledge, critical phenomena and metastability have not yet been consistently studied with this approach.[25–29]

Here, we present a simple, physically realizable electronic network which displays some behaviours reminiscent of criticality and metastability in biological neural networks. The key circuit element is the glow lamp, a miniature neon-argon gas discharge tube once widely utilized in logic and oscillating circuits. This device behaves hysteretically, transitioning to "on" state (finite resistance, light emission) above a striking voltage and to "off" state (near-infinite resistance, no light emission) below a lower extinction voltage. These voltages depend on physical parameters including electrode spacing and composition, gas composition and pressure, presence of ionization sources. Close to the striking and extinction voltages, corresponding transitions (thereafter termed breakdown and recovery) are stochastic with probability determined by the applied voltage, a phenomenon central to the system considered herein.[30,31] Testament to the value of the glow lamp as a non-linear circuit element comes from the fact that electronic chaos was originally discovered (though not recognized as such) by van der Pol in a glow lamp oscillator, and from his early models of neural dynamics which used it in approximating the Hodgkin–Huxley equations.[32,33]

By combining capacitive coupling with the glow lamp's hysteretic dynamics, nodes in the proposed circuit effectively accumulate energy and then dissipate it abruptly once a threshold is reached, in turn causing other nodes to do the same. This behaviour resembles integrate-and-fire in biological neurons, and the physical underpinnings of other well-known critical phenomena such as earthquakes, forest fires, and nuclear chain reactions.[2,34–36] As discussed below, critical phenomena are observed near the edges of the metastable region in a first-order (discontinuous) phase transition, rather than at a second-order (continuous) phase transition as is more often the case.

II. CIRCUIT DESCRIPTION AND EXPERIMENTAL SETUP

A. Circuit topology and principle of operation

The network consists of a 34×34 square lattice, wherein each node comprises a glow lamp connected between ground and a global DC control voltage V_s via a resistor of value R, and coupled to its four von Neumann neighbours via capacitors of value C (Figure 1(a)). This circuit is reminiscent of a well-known counter based on a glow lamps ladder, generalized to two dimensions.[30,37]

When all lamps are in the "off" state, node potentials obey the following dynamical equation (suitably adjusted for nodes along the perimeter):

$$\frac{\mathrm{d}}{\mathrm{d}t}v_{i,j} = \frac{1}{4}\frac{\mathrm{d}}{\mathrm{d}t}\left(v_{i-1,j} + v_{i+1,j} + v_{i,j-1} + v_{i,j+1}\right) + \frac{V_s - v_{i,j}}{4CR}, \quad (1)$$

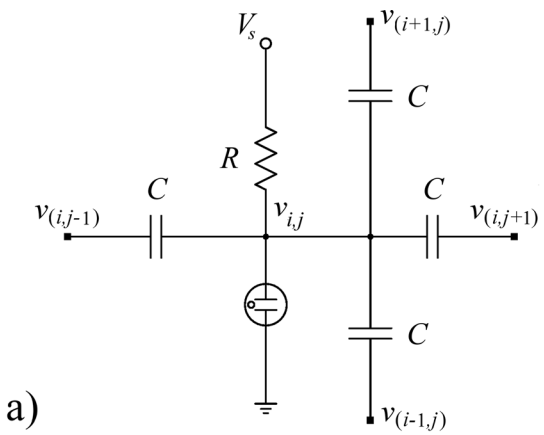

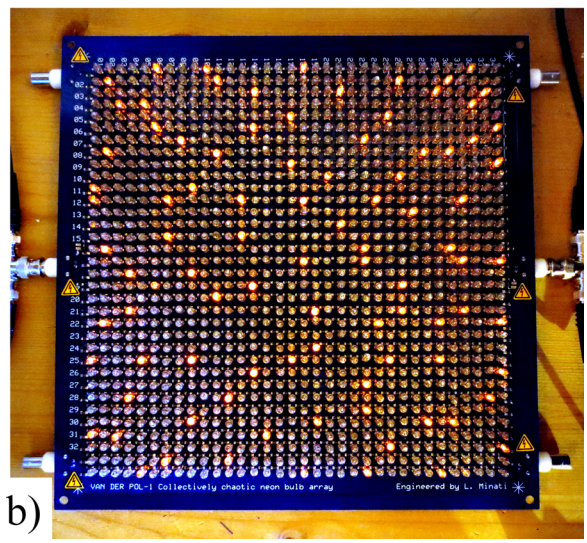

FIG. 1. Circuit description. (a) Circuit diagram of the two-dimensional square lattice node: a glow (neon) lamp, the potential at which is referred to as $v_{i,j}$, is connected to a global DC supply voltage V_s via a resistor of value R, and coupled via four capacitors of value C to its four von Neumann neighbours (each capacitor is shared between two nodes). R and C are fixed, whereas V_s is variable and serves as control parameter. (b) Top view of the 34×34 nodes circuit board, pictured while powered at 74.2 V.

where $v_{i,j}$ represents the potential at node i, j. Given sufficient time after a breakdown event (intended as rapid "off" → "on" → "off" transitions in a lamp's state, corresponding to a flash), node voltages return to equilibrium, i.e., $v_{i,j} \to V_s$, and further events are purely stochastic, their probability increasing with V_s. When breakdown occurs at a given node, its voltage drops because the corresponding lamp resistance becomes finite; since this change is rapid compared to the RC time constants in the lattice (≈10 μs vs. ≈10–100 ms), voltages at all other nodes also drop. While a lamp is in the "on" state, a spatial gradient of node voltages and charge stored in the coupling capacitors is established, whose characteristics depends on the location and duration of the "on" state. Eventually, the lamp recovers, similarly causing a rise in all node voltages. The fundamental aspect of the present circuit is that during this process node voltages higher than the applied control voltage V_s are momentarily generated, enhancing the probability of further breakdown events relative to quiescence.

To gain insight into this mechanism, let us first consider the short RC chain in Figure 2(a), wherein V_s is the DC control voltage, v_0 is held at a constant potential $v_0 < V_s$ to represent a lamp in the "on" state at this site, and $v_1(0) = v_2(0) = v_0$ to represent the initial negative step due to breakdown. The dynamical equations for the potentials are

$$\begin{aligned} \frac{\mathrm{d}}{\mathrm{d}t}(v_2 - v_1) &= \frac{V_s - v_2}{CR}, \\ \frac{\mathrm{d}}{\mathrm{d}t}(v_1 - v_0) &= \frac{2V_s - v_1 - v_2}{CR}, \end{aligned} \tag{2}$$

whose solution is (assuming without loss of generality $V_s = 0$)

$$\begin{aligned} \frac{v_1(t)}{v_0} &= \frac{1}{1+\varphi^2} e^{-t/\tau_1} + \frac{\varphi^2}{1+\varphi^2} e^{-t/\tau_2}, \\ \frac{v_2(t)}{v_0} &= \frac{\varphi^3}{1+\varphi^2} e^{-t/\tau_2} - \frac{\varphi^{-1}}{1+\varphi^2} e^{-t/\tau_1}, \end{aligned} \tag{3}$$

where $\tau_1 = RC\varphi^2$, $\tau_2 = RC\varphi^{-2}$, and φ is the golden ratio. Charting these solutions reveals that $v_2 > v_1$; in particular, even neglecting the effect of lamp recovery as done in this case, a positive transient (overshoot) exceeding V_s is observed for v_2, the farthest lamp in the chain, but not for v_1, the nearest one (Figure 2(b)).

This effect generalizes to the two-dimensional lattice, wherein breakdown events induce travelling waves of voltage overshoot. Numerical simulations with the model described in supplementary material Section S1 A and Figure S2 confirm that at short delays after the generating event (arbitrarily assumed to last 2 ms), the largest overshoot is observed at the farthest nodes; for longer delays, the overshoot wave propagates back towards the originating node, becoming shallower but more persistent at short distances (Figures 2(c) and 2(d)).[38]

These results, together with the corresponding experimental observations in supplementary material Section S1 B and Figure S3, demonstrate that despite short-range structural coupling with first neighbours only, activity propagation can extend over much longer distances, comparable with lattice size.[38] This property is similar to synchronous-mode propagation of action potentials across synapses in biological neural networks.[39–41] Thus, the interactions are effectively long-range, as observed elsewhere, for instance, in regards to elastic interactions and fracture propagation, which implies that even for low dimensions the system dynamics is predicted to approximate mean-field behaviour.[42,43]

B. Circuit realization and data acquisition

The system was implemented on a custom-designed printed circuit board, whose fabrication files are provided as supplementary material,[38] and where 1156 glow lamps of model NE-2C were instantiated with a pitch of 1/3 in. (Figure 1(b)). On a subsample of 30 lamps, upon delivery, the DC striking and extinction voltages measured, respectively, 76.2 ± 0.8 V and 61.3 ± 0.6 V (mean ± standard deviation). Supply resistors and coupling capacitors, respectively, had values $R = 2.2 \times 10^6\ \Omega$ (accuracy 1%) and $C = 220 \times 10^{-9}$ F (accuracy 10%). As detailed in supplementary material Section S1 C, flashes were recorded optically by means of both (i) two CCD cameras, providing information about node location at a rate of 50 Hz, and (ii) a photodiode, providing no spatial information but a higher sampling rate of 20 kHz.[38] The entire event times dataset is available online, and raw video and waveforms are also available upon request.[44]

III. PHASE TRANSITION

A. Existence of two dynamical phases

To begin studying the effect of control voltage V_s, activity was measured while this parameter was swept between

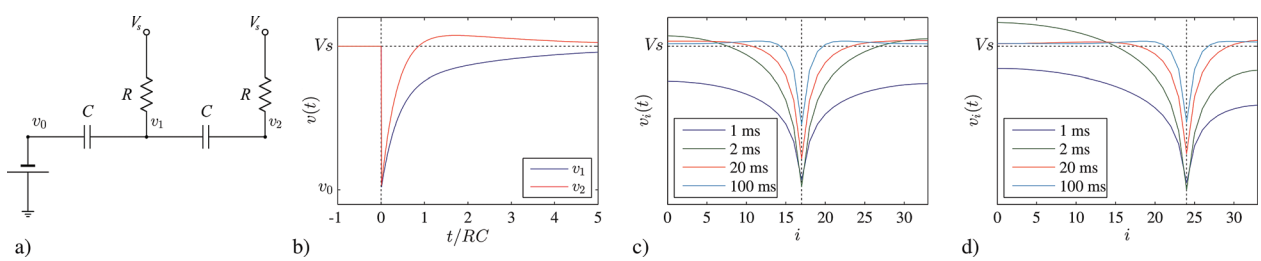

FIG. 2. Numerical simulations of voltage overshoot generation. (a) Simplified circuit, in the form of an RC ladder, representing three nodes v_0,v_1,v_2, with infinite-duration breakdown (lamp in "on" state) at node v_0, and (b) corresponding voltage time-series obtained from Eq. (3), demonstrating that a transient voltage overshoot, i.e., $v_2 > V_s$, is generated at the farthest node. (c) and (d) Corresponding simulations in the 34×34 lattice for 2 ms-long breakdown at two different locations ($j = 17$), obtained with the model described in supplementary material Section S1, showing that immediately after recovery the largest overshoot is observed at the farthest nodes, and a wave then propagates back towards the originating node, becoming shallower but more persistent at shorter distance.

73 and 75 V in steps of 0.1 V. For each setting, ≥50 measurements were taken in separate runs, each time reducing V_s to 71.5 V (quiescence) and increasing again it to the desired value at a rate of 0.1 V/s before data acquisition.

The event rate averaged over all nodes increased slowly, remaining around ≈0.01 Hz until $V_s \geq 74.1$ V, then abruptly increased, reaching ≈0.4 Hz (Figure 3(a)) and denoting the onset of self-sustained collective oscillation (corresponding voltage waveforms in supplementary material Figure S4(c)). The degree of spatial order (homogeneity) was quantified, expressed as $-\log_{10}(F_s)$, where F_s is the Fano factor (variance divided by average) of event counts calculated across all nodes after removal of radial gradient due to finite size; similar to rate, this parameter remained relatively stable then suddenly increased for $V_s \geq 74.1$ V, indicating transition to a more homogeneous spatial distribution (Figure 3(b)). The degree of temporal order (burstiness) was also quantified, as $-\log_{10}(F_t)$, where F_t is the Fano factor of event counts across non-overlapping 0.8 s—long windows (window width is not critical). For very small V_s, the system was near-quiescent and the event distribution was Poissonian; as V_s was increased, activity became more bursty, followed by an abrupt change for $V_s \geq 74.3$ V, past which the distribution of events suddenly became regular (under-dispersed with respect to Poissonian; Figure 3(c)).[45]

Predicated on these initial findings, representing the average over the entire observation window (≈50 s), we recorded the existence of two dynamical phases that we thereafter term Phases I and II, characterized, respectively, by low rate and low spatiotemporal order, and high rate and high spatiotemporal order.

B. Metastability and hysteresis

To gain further insight, rather than averaging over them we considered the existence of and transitions between Phases I and II during the observation window. Across runs, for V_s between 73.6 V and 74.3 V, both phases (separated at a threshold of 5 events/frame, which is not critical; see supplementary material Figure S5(a)) could be observed. Only the Phase I → II transition was directly observed, because the preset V_s values were always approached from below and, close to the transition, average Phase II lifetimes were longer than the observation window.

The probability of observing the Phase I → II transition peaked at $V_s = 74.2$ V (maximal variance) whereas for most runs at $V_s = 74.3$ V the system had already transitioned to Phase II before recording began (Figures 3(a)–3(c). At $V_s = 74.2$ V, the transition appeared as a gradual rate increase over a span ≈10 s (supplementary material Figure S5(a)) and in the majority of cases occurred approximately half-way during recording (supplementary material Figure S5(b)).

At this voltage, in Phase I, the distributions of inter-event interval (IEI) and number of active nodes per frame were approximately power-law and exponential, whereas in Phase II they were closer to normal, with average IEI ≈3 ms and number of active nodes per frame ≈10 (supplementary material Figures S5(c) and S5(d)), rendering this phase "crystal-like." The qualitative difference between the two phases at this control voltage setting is appreciable in representative frame sequences and rate maps (Figure 4).

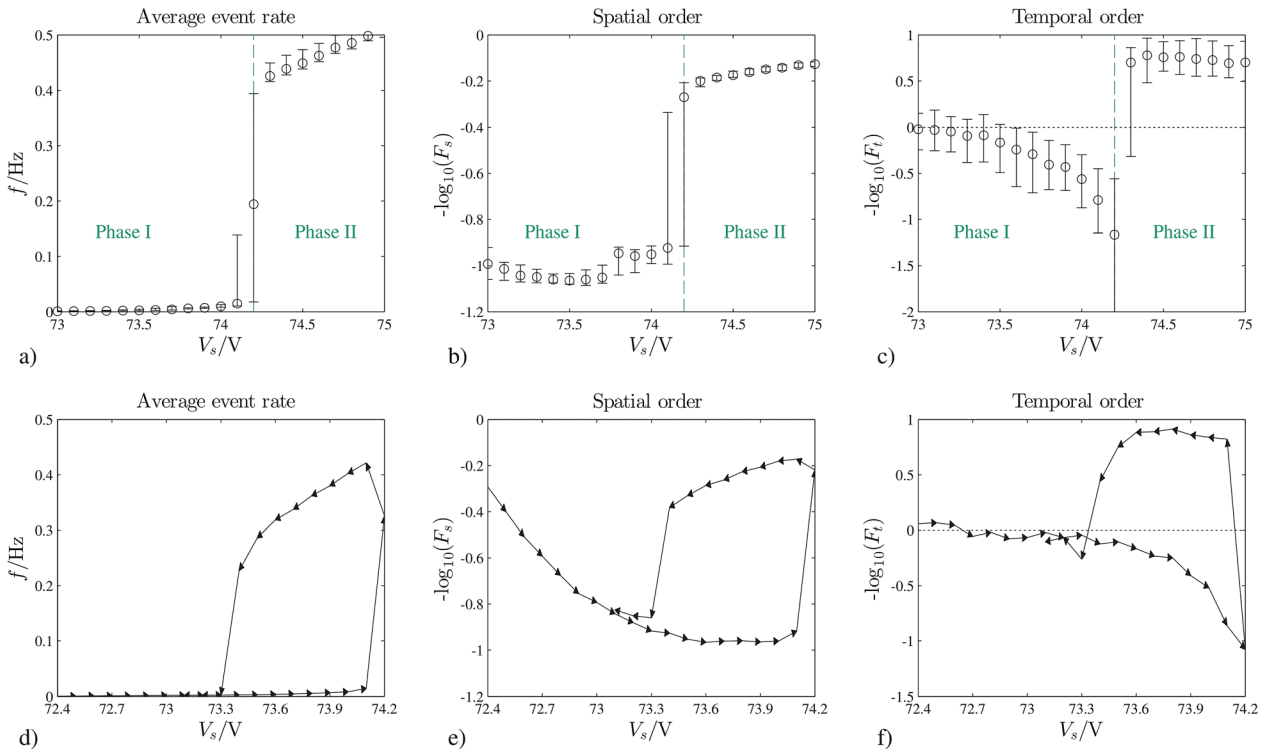

FIG. 3. Phase transition due to control voltage V_s. (a) Scatter plots (median ± 95% confidence interval) showing separate measurements taken between 73 V and 75 V. Around 74.2 V, transition between predominant low-rate low-order dynamics (Phase I) and high-rate high-order dynamics (Phase II) occurs, and inter-measurement variance is maximal. (b) Cycle plots representing continuous voltage sweep from 72.4 V (near-complete inactivity) to 74.2 V and back: hysteresis is evident as Phase I → Phase II transition ≈74.2 V and Phase II → Phase I transition ≈73.3 V.

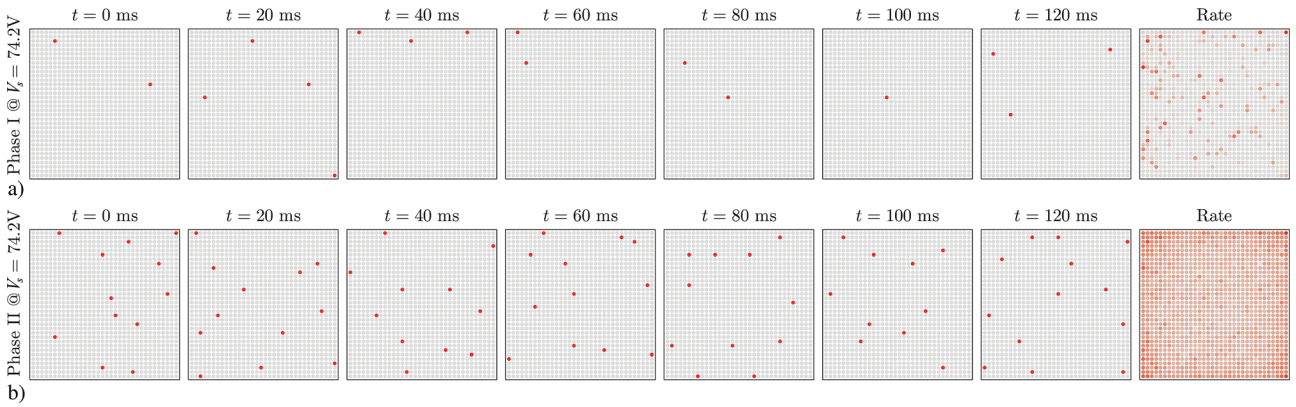

FIG. 4. Representative camera-frame sequences and event-rate spatial distribution at control voltage $V_s = 74.2$ V. (a) During Phase I, non-blank frames predominantly have a low event count (exponential-like distribution, see supplementary material Figure S5(d)), and the rate spatial distribution is markedly inhomogeneous. (b) During Phase II, frames on average contain ≈10 events (normal-like distribution, see supplementary material Figure S5(d)), and the rate spatial distribution is more homogeneous.

The above results were obtained in separate measurement runs, i.e., V_s was lowered until quiescence then raised again to the new V_s value before each recording. To reveal hysteresis in the Phase I ↔ II transition, a similar set of measurements was also acquired while cycling V_s over preset values without quenching activity between measurements. The cycle, from 72.4 V to 74.2 V and back to 73.1 V, was repeated 24 times. As above, the average event rate rose slowly then suddenly increased for $V_s \geq 74.2$ V (Phase I → II transition); it increased further as voltage was lowered one step to 74.1 V (due to longer time, hence greater cumulative probability of transition to Phase II) then decreased slowly, only transitioning back to low values for $V_s \leq 73.3$ V (Phase II → I transition; Figure 3(d)). The spatial and temporal order parameters followed a similar pattern (Figures 3(e) and 3(f)).

As detailed in supplementary material Section S1 A and Figures S2(a) and S2(b), analogous results were obtained in numerical simulations conducted with a simplified model, capturing the stochastic nature of transitions between lamp "on" and "off" states with probability dependent on applied voltage, but neglecting all fine details of lamp behaviour and inter-node differences due to component tolerances.[38]

C. Commentary

Power-law distributions as described in Section IV are frequently associated with second-order (continuous) phase transitions.[3] However, metastability and hysteresis unequivocally indicate that the transition between Phases I and II is a first-order (discontinuous) one. This apparent incongruence is resolved by considering that critical phenomena also emerge in first-order phase transitions as one enters the metastability region and approaches the spinodal curve. In practice, this requires changing the control voltage gradually in the absence of external perturbations, similarly to temperature in regards to obtaining super-heated and super-cooled water. Close to the spinodal, which in mean-field approximation denotes the limit of existence of the metastability region, transition precursors are observed which follow power-law scaling having a cut-off diverging to infinity on the spinodal itself; examples are found, for instance, in geophysical phenomena, breakdown of solids, and spontaneous network recovery.[42,43,46–48]

Assuming that interactions are long-range, in infinite size we expect infinite lifetime of the metastable states up to two spinodal voltages $V_s^{(1)}$ and $V_s^{(2)}$; otherwise, the metastable states have a finite lifetime decreasing to zero as one approaches these points. When the average lifetime overlaps the experimental observation window, corresponding "pseudo-spinodal" voltages $\hat{V}_s^{(1)}$ and $\hat{V}_s^{(2)}$, which are approximations of the underlying spinodal voltages, become apparent as observed above.[46]

In between $V_s^{(1)}$ and $V_s^{(2)}$ lies a third voltage at which average lifetime is equal between the two states. In our case, the system is inherently not in equilibrium because Phases I and II are dynamical, but it is helpful to consider that for an equilibrium system this point would correspond to the condition of equal free energy. Here, we could not measure this voltage because the duration of the states would be very long compared to the experimental observation window. Notably, this is not a critical voltage; hence, no critical phenomena are predicted to occur in its vicinity; instead, we expect divergence approaching the spinodal points.

IV. CRITICAL PHENOMENA

A. Branching parameter

In the metastable region below the upper spinodal voltage $V_s^{(2)}$, precursors of the spinodal transition are predicted as activity avalanches, wherein lamp breakdown events trigger descendants over a distance scale comparable to system size. As propagation is effectively long-range, critical behaviour at the spinodal point can be approached (see Section II A, supplementary material Section S1 B and Figure S3).[38]

To verify this, we computed the so-called "branching parameter" $\sigma(V_s)$, which represents how many descendants the voltage overshoot following a single event triggers on average. Below $V_s^{(2)}$, for rising V_s, this parameter is predicted to increase strictly monotonically because the quiescence potential approaches the average lamp breakdown voltage, elevating the probability that a given overshoot will trigger an event. While the branching parameter is usually considered

in regards to second-order transitions (e.g., branching process), it is also defined for first-order spinodal transition. In this case, it reaches the value $\sigma = 1$ at the transition but does not necessarily assume values larger than one, because instead of entering a "super-critical" regime, the system transitions discontinuously to a different phase (Phase II in our case).[34,42,43]

We calculated $\sigma(V_s)$ at $V_s = 73.8,\ldots,74.2$ V until transition to Phase II was detected ($\geq$560 recording runs per voltage setting in this range). Similarly to a study demonstrating critical branching in the spontaneous activity of cultured neuronal networks, we defined

$$\sigma = \sum_{d=0}^{n_{\max}} d \times p(d), \tag{4}$$

where the number of descendants d was generalized to multiple ancestors according to

$$d = \text{round}\left(\frac{n_d}{n_a}\right), \tag{5}$$

where n_a and n_d are, respectively, the number of active lamps in a given time-bin (see Subsection IV B) and in the following one during an avalanche.[4,49] The probability of observing a given number of descendants was calculated as

$$p(d) = \frac{1}{n_{\text{bins}}} \sum_{\text{bins}} \left(\frac{n_{\sum a|d}}{n_{\sum a}} \frac{n_{\max} - 1}{n_{\max} - n_p} \right), \tag{6}$$

where $n_{\sum a}$ is the total number of ancestors, $n_{\sum a|d}$ the number of ancestors having d descendants, $n_{\max} = 1156$ system size, and n_p the number of events observed in the previous bins within the avalanche, to approximately correct for refractoriness (see Ref. 4).

As predicted, σ increased with V_s, from $\sigma > 0.6$ at $V_s = 73.8$ V to $\sigma > 0.9$ at $V_s = 74.2$ V, in line with criticality at the spinodal voltage (Figure 5(a)), which we could not reach due to finite lifetime of Phase I. Above the spinodal voltage, we observed $\sigma \approx 1$ because short-range inhibition (see Section II B, supplementary material Section S1 B and Figure S3) effectively clamped the maximum event rate: the system did not become super-critical, but transitioned to Phase II, having markedly different dynamical properties (supplementary material Figures S5(c) and S5(d)).[38]

We underline that even though $\sigma \approx 1$ both in Phase I close to the spinodal voltage and in Phase II, the underlying dynamics were different. In Phase I, the number of descendants was highly variable, and finite avalanches and fractal structure were detected (see Subsections IV B and IV C); contrariwise, in Phase II the number of descendants was stable, without evidence of critical phenomena (i.e., activity effectively constituted a single endless avalanche). This illustrates the difference between super-critical dynamics (expected in second-order phase transition, and occasionally observed in biological neural networks) and discontinuous transition to a different phase (observed here).[2,4]

In Phase I at $V_s = 74.2$ V, the activity was near-critical, similarly to observations in cultured neuronal networks,

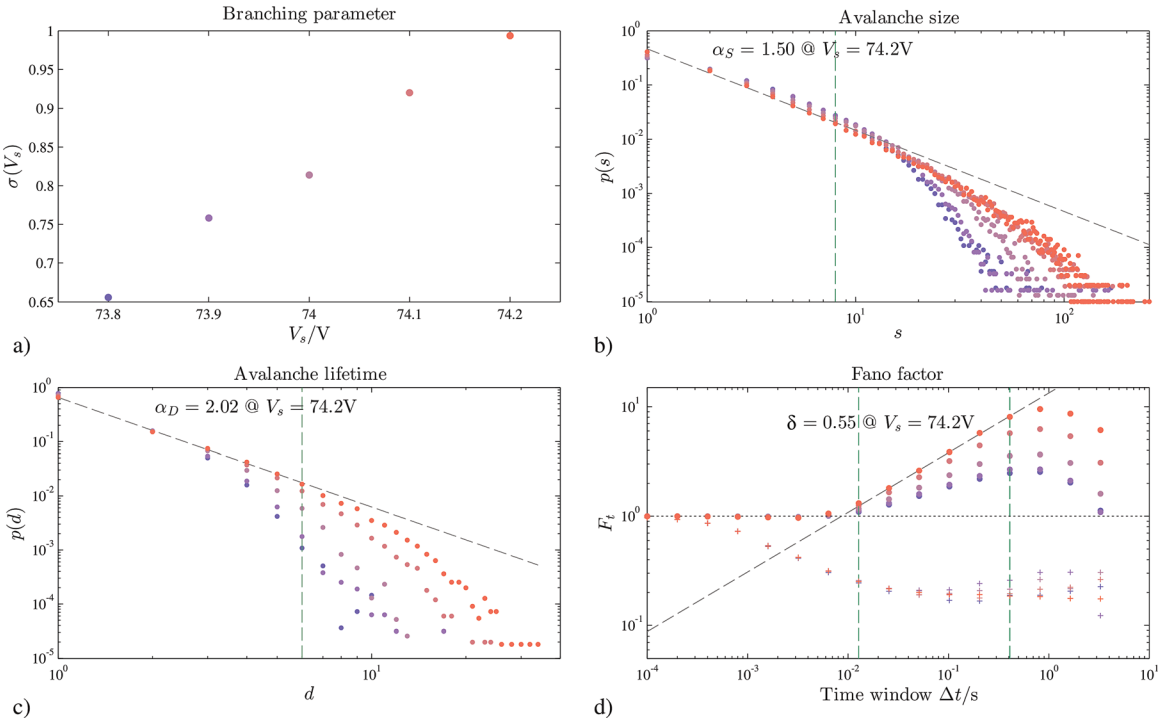

FIG. 5. Emergence of critical phenomena in Phase I for control voltage $V_s \to 74.2$ V. (a) The average branching parameter σ, representing number of descendants per ancestor event, monotonically approaches unity (here and in panels (b)–(d), colour denotes control voltage). (b) The avalanche size diverges, the underlying distribution increasingly resembling a power-law with $\alpha_S = 3/2$. (c) The avalanche duration also diverges, the underlying distribution increasingly resembling a power-law with $\alpha_D = 2$. Even at 74.2 V, exponential cut-off with respect to power-law (dashed gray lines) remains clearly visible for both distributions; the green dashed lines denote chosen upper limit for line-fitting (see text). (d) Filled dots and crosses represent the Fano factor in Phases I and II which are, respectively, over- and under-dispersed at all scales with respect to Poissonian distribution (unity, fine-dashed black line). In Phase I particularly at 74.2 V, a power-law increase (dashed gray line) is evident over a scaling range, confirming emergence of fractal behaviour.

even though here criticality was the result of external tuning rather than self-organized. It is noteworthy that operation close to criticality seem to be the preferential state at which biological neural networks combine maximization of information transmission and capacity with stability requirements.[2,4,5]

B. Avalanche size and duration divergence

Approaching from below the spinodal voltage $V_s^{(2)}$, with $\sigma \to 1$, the avalanche size s (number of nodes involved) and duration d are predicted to diverge, their distributions approaching power laws with characteristic exponents depending only on the universality class of the transition.

To test this hypothesis, we searched for probability distributions $p(s) \approx s^{-\alpha_S}$ and $p(d) \approx d^{-\alpha_D}$ in the experimental data acquired, respectively, with the cameras and photodiode. The avalanches were identified as event bursts, separated by a minimum quiescence time Δt which was empirically set, separately for each V_s value, to the average inter-event interval as discussed in Ref. 4; further, the avalanche durations were normalized to $d = t/\Delta t$.

The resulting charts had the characteristic appearance expected for a sub-critical process, wherein the distributions converged to a power-law largely independent of V_s for small size and short duration, with a prominent cut-off shifting towards larger size and longer duration for increasing V_s. For $V_s = 74.2$ V (>1000 recording runs, $\Delta t = 53.3$ ms), line-fitting the initial part of the distributions yielded $\alpha_S = 1.50$ and $\alpha_D = 2.02$ (Figures 5(b) and 5(c)). These experimental exponents are in agreement with $\alpha_S = 3/2$ and $\alpha_D = 2$ expected for the critical branching process and self-organized criticality, and observed for mature preparations of cultured dissociated neurons, isolated slices, and entire brains.[2,4–9,34,50,51] However, in our case, the exponents were observed at spinodal instability of a first-order transition. This is consistent, at least in regards to avalanche sizes, with the exponent found in other systems with a first-order transition, such as breakdown in fracture processes, random fuse model, and the "democratic fibre bundle model" (DFBM).[42,51,52] The same $\alpha_S = 3/2$ is also found in the long-range Ising model on the spinodal lines, with a suitable definition of the clusters.[53]

To further check the agreement of our measurements with $\alpha_S = 3/2$ and $\alpha_D = 2$, we performed a form of data collapse analysis over all size and duration distributions determined for $V_s = 73.8,\ldots,74.2$ V; while the cut-off (here assumed exponential) is expected to depend also on system size, this was not taken into account, since we could not alter it experimentally. Following Ref. 43 and the exactly solvable case of the DFBM, we fit to the data distributions of the form $p(s,V_s)$ and $p(d,V_s)$, with the scaling function $p(s,V_s) = s^{-\alpha} e^{s(V_s - V_s^{(2)})^{\kappa}}$ with $\alpha = 3/2$ and $\kappa = 1$ for size, and an analogous function for duration with $\alpha = 2$.[43,52,54] Applying the trust-region method with multiple restarts to $\log(p)$, for size we obtained $R^2 = 0.98$ and $V_s^{(2)} = 74.33$ V, whereas for duration $R^2 = 0.96$ and $V_s^{(2)} = 74.36$ V(data not shown). These results corroborate the conclusion that $\alpha_S = 3/2$ and $\alpha_D = 2$ for this system, and are in keeping with the observation that Phase I had a very short lifetime at $V_s = 74.3$ V. We additionally confirmed the α_S estimate with respect to array scale by recalculating this exponent while masking out half of the events using checkerboards having pitch 1, 2, 4, 8, and 16, which yielded α_S within [1.50,1.54].[4] Avalanching in accordance to $\alpha_S = 3/2$ and $\alpha_D = 2$ was also observed in numerical simulations with the simplified model, as described in supplementary material Section S1 A and Figures S2(c) and S2(d).[38]

Our results are therefore consistent with a transition in the same universality class of breakdown in disordered media, or the transition in the DFBM or in the long-range Ising model on the spinodal lines, that show power laws in the distributions of avalanches at the spinodal instability of a first-order transition.[43,52,54,55]

Attempts were also made to detect recurrent spatiotemporal avalanching patterns which would bear similarity to the "repertoires" found for neural cultures, using hierarchical trees and other classification techniques, but these were not found (data not shown).[56]

C. Fractal structure

Another aspect of critical phenomena is fractal behaviour, leading to generation of long-range correlated time series.[15,45,57] As breakdown events constitute a point process, we investigated this aspect by calculating the Fano factor, i.e., count variance divided the mean, over a span of timescales (0.1 ms–3 s, windowing the signal in powers of two). For a Poissonian process, by definition the Fano factor is unitary; it becomes larger for temporally clustered events (over-dispersed, such as avalanches) and smaller in the presence of regularity (under-dispersed). For a fractal process, the Fano factor is predicted to exhibit power-law scaling over a suitable range of temporal scales.[45,57]

As expected given the qualitative features of activity (Figure 4, supplementary material Figures S5(c) and S5(d)), in this experiment, the Fano factor was positive in Phase I and negative in Phase II, at all control voltage values $V_s = 73.8,\ldots,74.2$ V (Figure 5(d)).[38] Approaching the spinodal voltage $V_s^{(2)}$ in Phase I, power-law scaling became increasingly evident in the range of 13–400 ms; at $V_s = 74.2$ V, the corresponding exponent $\delta = 0.55$ with $R^2 > 0.99$. This result confirms critical behaviour, without entailing assumptions about the threshold Δt used to delineate avalanches. The value found for δ is also not very distant from $\delta \approx 0.78$ observed in mature cultures of dissociated cortical neurons.[6]

V. DISCUSSION AND CONCLUSION

We illustrated a circuit wherein energy storage in the coupling capacitors together with the glow lamp's probabilistic and hysteretic behaviour lead to dynamics similar to other processes, such as earthquakes, forest fires, and spike propagation in neurons, where elements gradually accumulate energy then abruptly release it, causing others to do the same.[2,34–36] Despite first-neighbour structural coupling, interactions in this system are effectively long-range, enabling

the observation of phenomena that are characteristic of mean-field approximation.

By varying the DC control voltage applied globally to the array, two dynamical phases were observed, the transition between them being discontinuous and hysteretic, hence first-order. In the metastable region of this transition, approaching to the spinodal critical precursors of the transition emerge, including divergence of avalanche size and duration, and long-term temporal correlation. The qualitative and quantitative features of these phenomena overlap well with experimental evidence in neuronal systems, despite obviously different underlying physical mechanisms, spatio-temporal scale, and network size.[2,4–9]

However, in biological neural circuits, critical behaviour emerges without external tuning, presumably due to a internal self-regulation mechanism that maintains the system close to the critical point (self-organized criticality).[15–17] Contrariwise, in this circuit, (near) critical behaviour is observed only when driving the system near the spinodal point by externally tuning the control parameter (supply voltage). While in neural circuits plasticity (and other adaptive mechanisms) support self-organization, here possibilities for self-organization are constrained because the structural connectivity and circuit parameters are fixed.

In biological neural circuits, critical phenomena can be observed for very long time-spans, compatible with the lifetime of the system itself; contrariwise, here critical phenomena arise during a metastable state: approaching the spinodal point, while the avalanche size and duration diverge, the lifetime of the metastable state decreases, eventually making experimental observation impossible. An external controller to restore criticality after transition to the stable state could be devised, but this would not alter the fundamental fact that the lifetime of the metastable state is finite, which is at odds with seemingly "persistent" criticality in neurophysiological data.[2,4–9]

Indeed, biological neural circuits are widely deemed to be governed by a second-order phase transition, whereas critical phenomena in this circuit are observed close to a first-order transition.[2,5] Further experimental study of phase transitions in biological neural networks is anyway motivated, particularly because reconciling the hypothesis of a second-order phase transition with evidence of metastability is not trivial. While it is not easy to manipulate "control parameters" of intact brains, neurons cultured *in-vitro* provide a convenient experimental platform to investigate system response to a multitude of biochemical control parameters (e.g., excitation/inhibition ratio), making it possible to search for hysteresis and other hallmarks, allowing differentiation between a first- and a second-order transition.

While in this experiment glow lamps were connected in a lattice, biological neural networks, even those spontaneously forming from dissociated neurons in an artificial environment, have complex architecture, their structure being significantly modular, small-world and scale-free.[2,58,59] Future work should consider the behaviour of this circuit in more ecologically-relevant topologies; while interactions were primarily long-range, short-range effects were also observed, and these could lead to dynamical differences depending on connectivity. In particular, in biological neural networks, avalanches seemingly follow "repertoires" of activity, associated with network maturity and integrity; by contrast, in this experiment, the avalanches appeared purely stochastic.[56] We conjecture that a structured repertoire could emerge even in this circuit given a richer connectivity structure. It is also worthwhile to consider how the emergent properties of this system are altered by gradual degeneration of structural connections.

Overall, these experimental results reinforce the capabilities of physical networks of electronic oscillators to recapture aspects of *in-vivo* and *in-vitro* neural dynamics. More generally, this observation of critical phenomena in a first-order phase transition is rare in electronic systems; hence, the proposed circuit may open up opportunities for experimental work in this area.

ACKNOWLEDGMENTS

The authors are grateful to Antonio Coniglio, Lucilla De Arcangelis, and Jorge Jovicich for fruitful discussions and feedback. These experimental activities were initiated and entirely funded by L.M. personally and conducted on own premises. L.M. gratefully acknowledges consulting funding from Scienze Mente-Cervello (Trento, Italy) for non-linear analysis of signals recorded in cultured neuronal networks.

[1]D. J. Amit, *Modeling Brain Function: The World of Attractor Neural Networks* (Cambridge University Press, 1989).
[2]D. Plenz, E. Niebur, and H. G. Schuster, *Criticality in Neural Systems* (Wiley, Hoboken, NJ, USA, 2014).
[3]L. D. Landau and E. M. Lifshitz, *Statistical Physics Part I* (Butterworth-Heinemann, Oxford, UK, 1980).
[4]J. M. Beggs and D. Plenz, J. Neurosci. **23**, 11167 (2003).
[5]D. R. Chialvo, Nat. Phys. **6**, 744 (2010).
[6]C. Tetzlaff, S. Okujeni, U. Egert, F. Wörgötter, and M. Butzm, PLoS Comput. Biol. **6**, e1001013 (2010).
[7]N. Friedman, S. Ito, B. A. Brinkman, M. Shimono, R. E. DeVille, K. A. Dahmen, J. M. Beggs, and T. C. Butler, Phys. Rev. Lett. **108**, 208102 (2012).
[8]E. Tagliazucchi, P. Balenzuela, D. Fraiman, and D. R. Chialvo, Front. Physiol. **3**, 15 (2012).
[9]P. Massobrio, L. de Arcangelis, V. Pasquale, H. J. Jensen, and D. Plenz, Front. Syst. Neurosci. **9**, 22 (2015).
[10]O. Kinouchi and M. Copelli, Nat. Phys. **2**, 348 (2006).
[11]A. J. Hudspeth, F. Jülicher, and P. Martin, J. Neurophysiol. **104**, 1219 (2010).
[12]W. L. Shew, H. Yang, S. Yu, R. Roy, and D. Plenz, J. Neurosci. **31**, 55 (2011).
[13]W. Shew and D. Plenz, Neuroscientist **19**, 88 (2013).
[14]S. H. Gautam, T. T. Hoang, K. McClanahan, S. K. Grady, and W. L. Shew, PLoS Comput. Biol. **11**, e1004576 (2015).
[15]P. Bak, C. Tang, and K. Wiesenfeld, Phys. Rev. Lett. **59**, 381–384 (1987).
[16]J. Hesse and T. Gross, Front. Syst. Neurosci. **8**, 166 (2014).
[17]M. Rybarsch and S. Bornholdt, PLoS One **9**, e93090 (2014).
[18]D. Durstewitz, J. K. Seamans, and T. J. Sejnowski, Nat. Neurosci. **3**, 1184 (2000).
[19]C. D. Brody, R. Romo, and A. Kepecs, Curr. Opin. Neurobiol. **13**, 204 (2003).
[20]S. Scarpetta and A. de Candia, PLoS One **8**, e64162 (2013).
[21]E. Tognoli and J. A. Kelso, Neuron **81**, 35 (2014).
[22]C. Haldeman and J. M. Beggs, Phys. Rev. Lett. **94**, 058101 (2005).
[23]J. Pu, H. Gong, X. Li, and Q. Luo, Sci. Rep. **3**, 1081 (2013).
[24]A. Levina, J. M. Herrmann, and T. Geisel, Phys. Rev. Lett. **102**, 118110 (2009).
[25]C. Mead, *Analog VLSI and Neural Systems* (Addison-Wesley, Boston, MA, USA, 1989).

[26]E. Chicca, F. Stefanini, C. Bartolozzi, and G. Indiveri, Proc. IEEE **102**, 1367 (2014).
[27]L. Minati, Chaos **24**, 043108 (2014).
[28]L. Minati, P. Chiesa, D. Tabarelli, L. D'Incerti, and J. Jovicich, Chaos **25**, 033107 (2015).
[29]L. Minati, Chaos **25**, 123107 (2015).
[30]C. R. Dougherty, T. D. Foulke, J. D. Harden, T. L. Hewitt, F. N. Peters, R. D. Smith, and J. W. Tuttle, *Glow Lamp Manual*, 2nd ed. (General Electric Company, Cleveland, OH, USA, 1966).
[31]J. B. Dance, *Cold Cathode Tubes* (Iliffe, London, UK, 1968).
[32]M. P. Kennedy and L. O. Chua, IEEE Trans. Circuits Syst. **33**, 974–980 (1986).
[33]F. Hoppensteadt, Math. Biosci. **245**, 56 (2013).
[34]T. E. Harris, *The Theory of Branching Processes* (Dover, New York, USA, 1989).
[35]B. Drossel and F. Schwabl, Phys. Rev. Lett. **69**, 1629 (1992).
[36]I. G. Main, Bull. Seismol. Soc. Am. **85**, 1299 (1995).
[37]J. Manley and E. Buckley, Electronics **23**, 84 (1950).
[38]See supplementary material at http://dx.doi.org/10.1063/1.4954879 for additional results, figures and board design materials.
[39]M. Diesmann, M. O. Gewaltig, and A. Aertsen, Nature **402**, 529 (1999).
[40]A. D. Reyes, Nat. Neurosci. **6**, 593 (2003).
[41]A. Kumar, S. Rotter, and A. Aertsen, J. Neurosci. **28**, 5268 (2008).
[42]S. Zapperi, P. Ray, H. E. Stanley, and A. Vespignani, Lect. Notes Phys. **567**, 452 (2001).
[43]S. Zapperi, P. Ray, H. E. Stanley, and A. Vespignani, Phys. Rev. Lett. **78**, 1408 (1997).
[44]See http://www.lminati.it/listing/2016/a/ for full set of experimental data (event time series).
[45]M. A. Buice and J. D. Cowan, Progr. Biophys. Mol. Biol. **99**, 53 (2009).
[46]D. W. Heermann, W. Klein, and D. Stauffer, Phys. Rev. Lett. **49**, 1262 (1982).
[47]J. B. Rundle, W. Klein, D. L. Turcotte, and B. D. Malamud, Pure Appl. Geophys. **157**, 2165 (2000).
[48]A. Majdandzic, B. Podobnik, S. V. Buldyrev, D. Y. Kenett, S. Havlin, and H. Eugene Stanley, Nat. Phys. **10**, 34 (2014).
[49]J. X. de Carvalho and C. P. Prado, Phys. Rev. Lett. **84**, 4006 (2000).
[50]C. Tang and P. Bak, J. Stat. Phys. **51**, 797 (1988).
[51]S. Zapperi, L. K. Baekgaard, and H. E. Stanley, Phys. Rev. Lett. **75**, 4071 (1995).
[52]D. Sornette, J. Phys. I Fr. **2**, 2089 (1992).
[53]D. W. Heermann, A. Coniglio, W. Klein, and D. Stauffer, J. Stat. Phys. **36**, 447 (1984).
[54]S. Zapperi, P. Ray, H. E. Stanley, and A. Vespignani, Phys. Rev. E **59**, 5049 (1999).
[55]K. Lauritsen, S. Zapperi, and H. E. Stanley, Phys. Rev. E **54**, 2483 (1996).
[56]J. M. Beggs and D. Plenz, J. Neurosci. **24**, 5216 (2004).
[57]A. L. Barabási and H. E. Stanley, *Fractal Concepts in Surface Growth* (Cambridge University Press, 1995).
[58]O. Sporns, *Networks of the Brain* (The MIT Press, Cambridge, MA, USA, 2009).
[59]J. H. Downes, M. W. Hammond, D. Xydas, M. C. Spencer, V. M. Becerra, K. Warwick, B. J. Whalley, and S. J. Nasuto, PLoS Comput. Biol. **8**, e1002522 (2012).